Lithium acetate modified PU/graphene composites as separator for advanced Li-ion batteries

Yong Jiang[1,2] ✉, *Cai Lu*[1], *Xing Liu*[1], *Yunhong Jiang*[1], *Yanhuai Ding*[1,2]

[1]*College of Civil Engineering & Mechanics, Xiangtan University, Hunan 411105, People's Republic of China*
[2]*Institute of Rheological Mechanics, Xiangtan University, Hunan 411105, People's Republic of China*
✉ *E-mail: jiangy@xtu.edu.cn*

Published in Micro & Nano Letters; Received on 24th May 2019; Revised on 12th November 2019; Accepted on 17th December 2019

Here lithium acetate modified PU/graphene composites were prepared from a simple electrospun method. The electrochemical properties, thermal stability, and mechanical properties of polyurethane (PU) separator have been improved remarkably by the addition of lithium acetate and graphene. The composite separator can maintain the dimension size even after being treated at 170°C for 1 h. High ionic conductivity of 2.47 mS·cm^{-1} can be reached. The results show that the as-prepared lithium acetate modified PU/graphene separator is a promising candidate for commercial polyolefin separators.

1. Introduction: Lithium-ion batteries (LIBs) have been widely used as the power source for portable electronic devices and electric vehicles due to their high energy density, and excellent cycle performance [1–6]. Undoubtedly, the electrochemical properties of the LIBs were mainly determined by the electrode materials [7–9]. However, battery separator plays a key role by protecting LIBs from short circuit and overcharge [10–18]. A good separator should meet the requirements of suitable thickness, high thermal stability, and high Li^+ ion transmission rate [19, 20]. At present, porous polyolefin membranes consisted of polyethylene (PE), polypropylene (PP), and their blends such as PE–PP and PP–PE–PP, have been widely used as separators for LIBs. However, the poor wettability to electrolytes, low thermal stability, and low porosity hinder their applications in advanced LIBs [21]. Thus, high-performance separators need to be explored.

In recent years, electrospinning technique has been developed to fabricate porous separators from a variety of polar polymers like poly(vinylidene-fluoride) (PVDF) [22], polyacrylonitrile (PAN) [23], polyimide (PI) [24], poly(ethylene oxide) (PEO), poly (methyl methacrylate) (PMMA), and polyurethane (PU) [25, 26]. Among them, PU-based separator exhibits great potential for flexible energy storage applications. Electrospun PU composite separators such as PU@PEO [27], SiO_2@PEI@PU [28], PU@PVDF [29], and PU/PVDF@HFP [30] were reported. It has been demonstrated that combining with inorganic particles and other suitable polymers can improve the electrochemical performance of PU. Also, the thermal stability of PU is remarkably enhanced by the addition of inorganic particles. Due to its ultra-high-strength and thermal stability, graphene is a potential filler that can dramatically enhance the properties of polymer-based composites at a very low content. Lithium salts have been rarely used as additives to improve the electrochemical performance of the polyolefin separators. Here, graphene and lithium acetate were employed to increase the mechanical and electrochemical properties of electrospun PU separators. The synergistic effect from lithium acetate and graphene on the properties of electrospun PU separator was systematically investigated.

2. Experimental

2.1. Materials: PU was supplied by Shanghai BASF (China) Co, Ltd. Lithium acetate (LiAc) was purchased from Shanghai Macklin Biochemical Co, Ltd. N,N-dimethylformamide (DMF) and Tetrahydrofuran (THF) were obtained from Tianjin Hengxing Chemical Reagent Co, Ltd. The commercial separator used in the comparative study is a Celgard 2400 membrane with a thickness of 16 μm (Celgard, China). Graphene nanosheets were purchased from Suzhou Tanfeng Tech. Inc. Co. Ltd. All the as-received chemicals were used directly.

2.2. Fabrication of separators: Firstly, 3 g PU was put into a mixture of 10 ml DMF and 10 ml THF to get a 15 wt% PU solution. The solution was isolated from air and aged at room temperature for more than 12 h with continuous stirring. Then 9 mg graphene nanosheets and 45 mg LiAc were dispersed in the solution with vigorous stirring and ultrasonication. The electrospun LiAc modified PU/graphene and raw PU/graphene separator (denoted as PU/G/LiAc and PU/G) were fabricated by a commercially available electrospinning set-up (Beijing Ucalery Technology Development Co, Ltd., China). Firstly, the as-prepared solution was fed into a syringe. The high voltage for generating a polymer jet was set to 13–16 kV. The distance between the nozzle and the grounded collector was adjusted to 12 cm. Collector was rotated at a constant rate of 20 rpm and covered with tin foil for accepting PU fibres. After removing solvent residues in vacuum conditions for 12 h, the membranes were kept in a desiccator for further use.

2.3. Physical and electrochemical characterisations: The shrinkage of the samples after being treated at 170°C for 1 h is calculated by the following equation:

$$\text{Shrinkage}\,(\%) = \frac{A_0 - A}{A_0} \times 100\%$$

where A_0 and A represent the initial and final areas of the relevant membrane, respectively.

The porosity performance of the samples was evaluated by performing the n-butanol uptake measurements, and then calculated by the following equation:

$$\text{Porosity}\,(\%) = \frac{M_w - M_d}{\rho_b V_d} \times 100\%$$

where M_d and M_w are the weights of the electrospun fabrics before and after soaking (wet) in n-butanol for 2 h. ρ_b is the density of n-butanol, and Vd is the volume of the dry electrospun nanofibres.

The electrode-uptake capacity was evaluated by soaking the membrane in 1 M $LiPF_6$ dissolved in (EC/EMC/DMC) (1/1/1/, w/w/w), and then calculated by the following equation:

$$\text{Uptake}\,(\%) = \frac{W_w - W_d}{W_d} \times 100\%$$

where W_w and W_d are the weights of the separator before and after soaking in the electrolyte for 1 h, respectively.

Instron 5943 universal testing instrument (Instron Int. Ltd., USA) was used to test the mechanical properties of the electrospun membranes. The as-prepared separators were cut into 1×5 cm rectangular shapes then mounted vertically on the mechanical clamping device of the tensile tester. The tensile loading speed is 0.05 cm/min. All the samples were tested five times and then averaged as the final data. Thermal gravimetric analysis and differential thermal gravimetric analysis (TGA/DTG) were performed on a TA SDTQ600 instrument under the argon atmosphere.

The separator was sandwiched between a $LiFePO_4$ cathode and a lithium metal anode to assemble a half-cell configuration. A PARSTAT 2273 electrochemical working station was used to test the ionic conductivity (σ) of the relevant membranes by electrochemical impedance spectroscopy (EIS) over the frequency range from 0.1 to 1 MHz at a scan rate of 5 mVs^{-1}. The ionic conductivity can be calculated by the following equation:

$$\sigma = \frac{d}{R_b \cdot A}$$

where R_b, d and A represent the bulk resistance (Ω), thickness (cm) and effective area (cm^2) of the separator, respectively.

The CR2016 coin cells with PU/G/LiAc separator sandwiched between a $LiFePO_4$ cathode and a lithium metal anode were assembled in an Ar-filled glove box. At room temperature, the LAND 2001A system was used to determine the cycle performance of the separator. The galvanostatic measurements were performed in the potential window of 2.5–4.2 V at various *C*-rates ranging from 0.2 to 5.0 C.

3. Results and discussion: Typical SEM images of the PU/G/LiAc membrane are shown in Fig. 1, which reveals that the electrospun separators are composed of randomly oriented fibres that have diameters ranged from 300 to 700 nm. A three-dimensional network structure was formed in the membranes. Additionally, it can be found that the fibres have a smooth surface free of beads, which can provide fabrics with good mechanical properties. The interconnected pore structures can serve as reservoirs for the electrolyte storage. Obviously, high porosity can be expected in electrospun separators.

The stress–strain curves of PU/G with different *G* contents in a strain range of 0–200% are shown in Fig. 2*a*. In the initial region, the stress–strain curves of all the samples are overlapped. With the further increase in strain, the stress increases nonlinearly. By comparison, the PU separator with 0.3 wt% of graphene delivers the highest stress of 1.67 MPa under a strain of 200%. The results show that the mechanical properties of the PU separators have

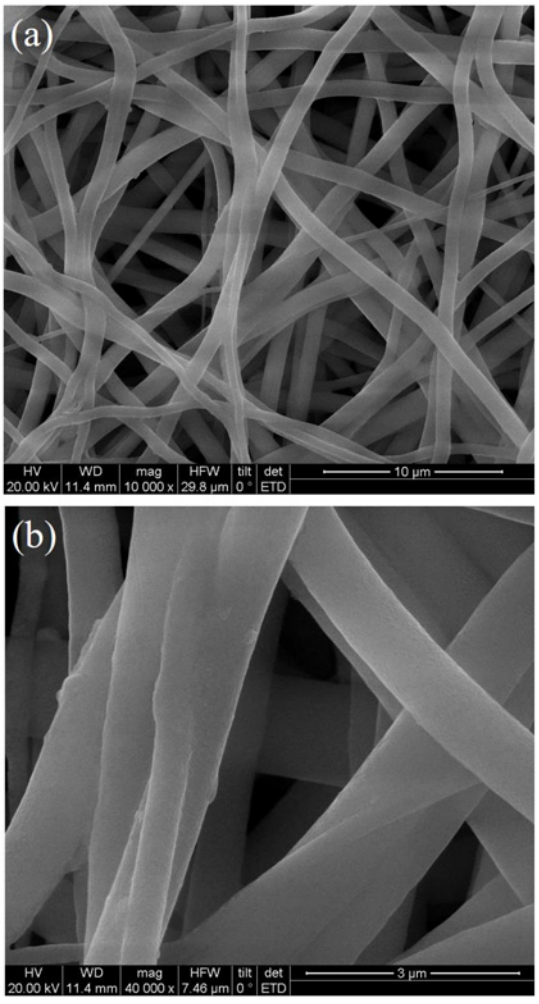

Fig. 1 *SEM images of PU/G/LiAc electrospun membranes*
a Porous structure of PU/G/LiAc separator
b Surface morphology of PU/G/LiAc nanofibers

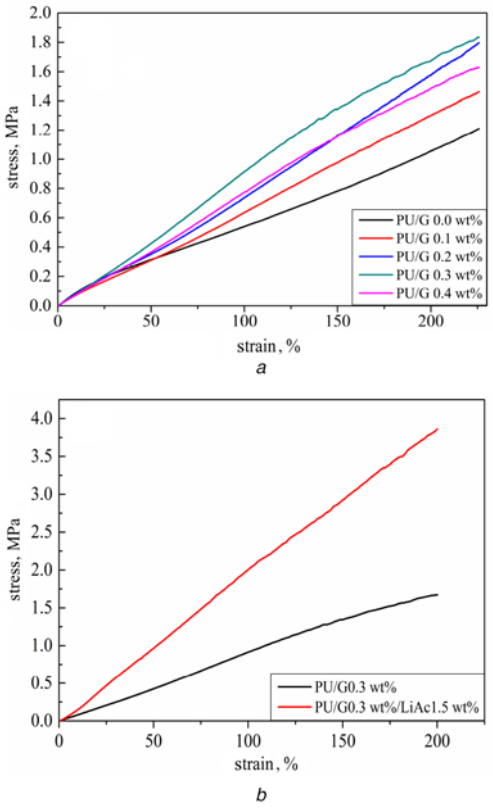

Fig. 2 *Mechanical behaviors of electrospun PU with different contents of G and LiAc*
a, *b* Stress–strain relationship of PU/G and PU/G/LiAc separators

doi: 10.1049/mnl.2019.0164

been enhanced by the addition of graphene. The theoretical tensile strength of graphene nanosheets is ~1.0 TPa, which is much higher than that of the PU matrix. With the increase in the graphene content, the tensile strength of the separators firstly increases and then decreases. The mechanical properties of the graphene-based composites are mainly determined by the dispersity of the nanosheets in the matrix. When the graphene content beyond the threshold value, the physical properties of the composites start to deteriorate due to the aggregation of graphene nanosheets. The effect of LiAc on the mechanical properties of PU/graphene was further investigated, as shown in Fig. 2*b*. Under a train of 200%, the corresponding stress of PU/graphene with 1.5 wt% LiAc reached 3.86 MPa. The well-dispersed LiAc in the PU matrix can further improve the tensile strength of the PU/graphene composites.

TG/DSC was used to evaluate the thermal stability of the separators. Fig. 3*a* shows the TG curves of different separators such as PP, PU, and PU/G/LiAc. TG analysis indicates that, until the temperature reached 300°C, the weight of PU/G/LiAc materials did no change. As can be observed from the DSC curves (Fig. 3*b*), the Celgard membrane separator indicates an endothermic peak at 150°C, which is the typical melting point of polypropylene [31].

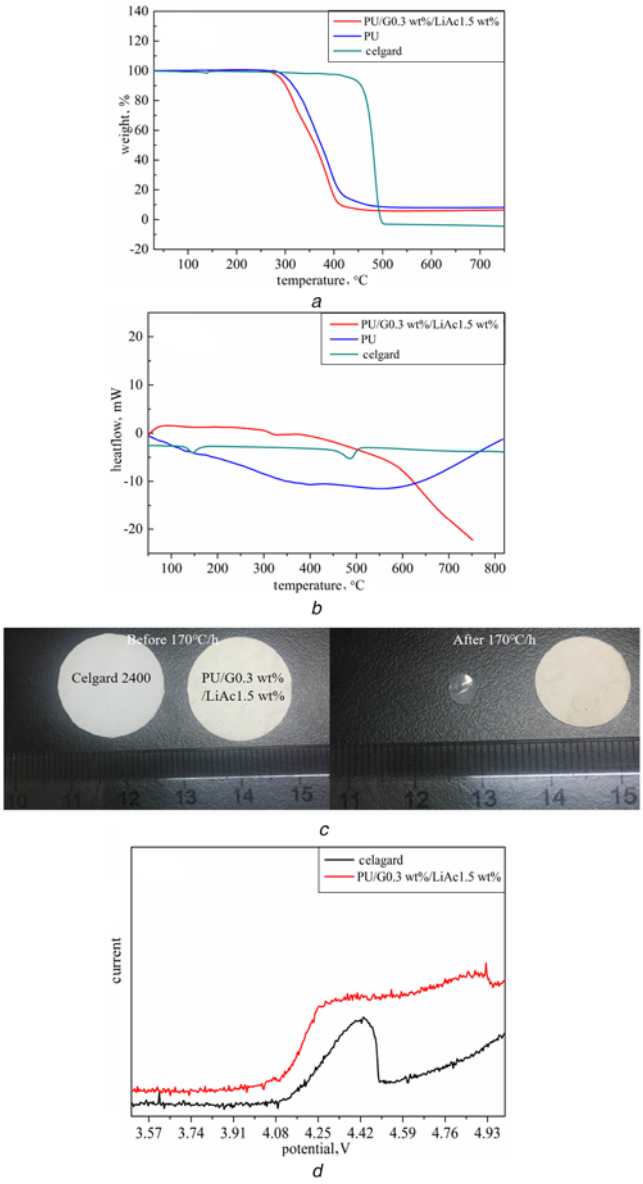

Fig. 3 *Thermal and electrochemical stability of as-prepared separators*
a, *b* TG/DSC curves of PU, PU/G/LiAc and Celgard
c Digital pictures of Celgard and PU/G/LiAc nanofibre membranes before (left) and after (right) heat-treated at 170°C for 1 h
d Electrochemical stability of Celgard and PU/G/LiAc separators

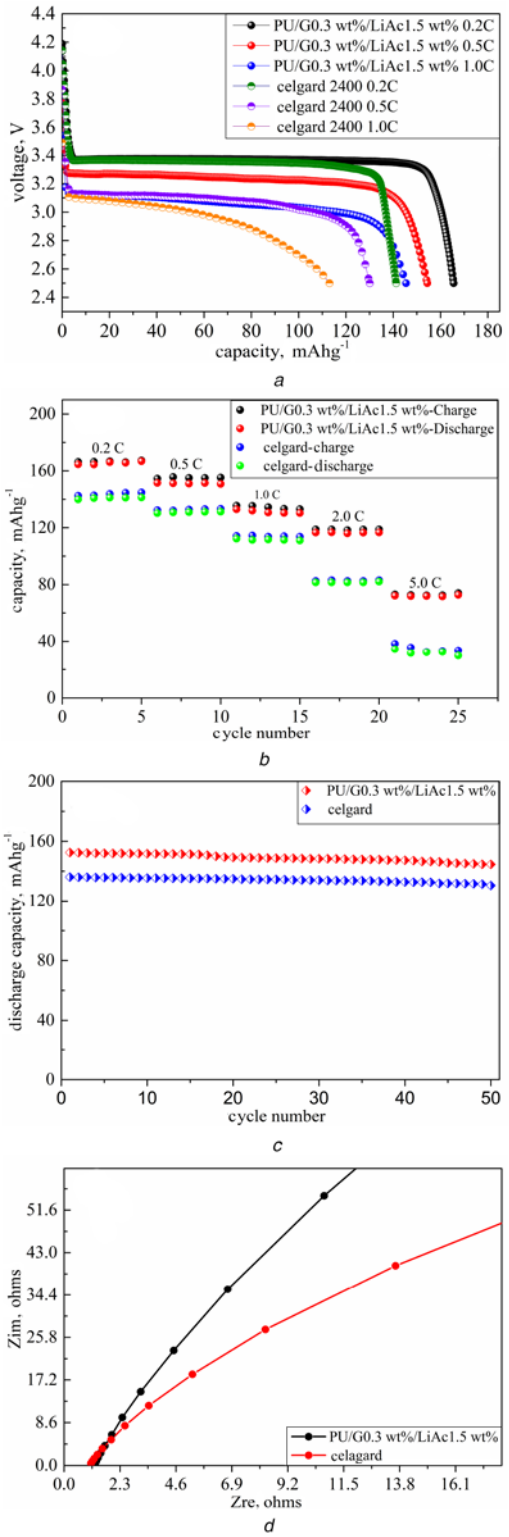

Fig. 4 *Electrochemical performance of the testing cells with electrospun separators and Celgard separator*
a Premier discharge curves of Li/$LiFePO_4$ cells assembled with PU/G/LiAc and Celgard separators
b Rate capabilities of Li/$LiFePO_4$ cells with Celgard and PU/G/LiAc separators
c Cycling performance of the testing cells at a low current density of 0.5 C
d AC impendence spectra of PU/G/LiAc and Celgard separators in stainless steel/separator/stainless steel system

Table 1 Electrolyte uptake, porosity and ionic conductivity of the PU/G/LiAc and the Celgard separators

Samples	Electrolyte uptake, wt%	Porosity, %	Ionic conductivity, $mS \cdot cm^{-1}$
Celgard	76.47	35.4	0.70
PU/G/LiAc	224.1	61	2.47

The curve of PU/G/LiAc is smooth and has no stronger peaks in it before 300°C, indicating better thermal stability. One of the best advantages of graphene materials is superior thermal stability. The graphene nanosheets can provide the PU nanofibres with a security barrier against the heat attack. Besides, the excellent thermal stability of the graphene nanosheets can effectively enhance the dimensional stability of the composite separators. Fig. 3*c* presents the digital pictures of the Celgard and PU/G/LiAc separators before and after being treated at 170°C for 1 h. Considerable thermal shrinkage was observed for Celgard separator, while there was only a 21.1% of shrinkage occurred in the PU/G/LiAc membrane. It can be expected that the PU/G/LiAc separator can significantly enhance the safety of LIBs. As revealed in Fig. 3*d*, the electrochemical decomposition does not take place in PU/G/LiAc separator until the test voltage increases up to 4.3 V.

Fig. 4 shows the discharge curves of the unit cells assembled with different separators in the potential range of 2.5/4.2 V at current densities of 0.2, 0.5, and 1 C. As shown in Fig. 4*a*, a very stable voltage plateau can be obtained for both the two samples. With the increase in current density, the discharge capacity decreased gradually. A shift of the plateau to a relatively low voltage is observed, which can be ascribed to the polarisation. By comparison, the testing cell with PU/G/LiAc separator can deliver a higher discharge capacity than that of the testing cell with Celgard separator. A specific discharge capacity of 164.59, 151.95, and 132.96 $mAhg^{-1}$ can be obtained at a current density of 0.2, 0.5, and 1.0 C, respectively. Compared to Celgard separator, the testing cell with PU/G/LiAc separator exhibits excellent rate capability at the current density from 0.2 to 5.0 C (Fig. 4*b*). A specific discharge capacity of ~70 $mAhg^{-1}$ can be delivered even at a high discharge current density of 5 C. As we expected, at 0.5 C, the testing cell with the PU/G/LiAc separator exhibits good cycling performance (Fig. 4*c*). After 50 cycles, a specific discharge capacity of 144.68 $mAhg^{-1}$ can be obtained, about 95% of the initial discharge capacity. Nyquist plots of Celgard and PU/G/LiAc membranes soaked with electrolyte were shown in Fig. 4*d*. The intercepts on the real-axis of Celgard and PU/G/LiAc membranes were 1.118 and 1.2987 Ω, respectively. Although the PU/G/LiAc separator exhibits slightly higher bulk resistance than the routine separator, the ionic conductivity of the separator of PU/G/LiAc exceeds that of the routine separator [18, 32]. The high electronic conductivity of graphene is beneficial to decrease the bulk resistance of the composite separator. However, due to the very small fraction of the graphene, the composite separator is still electrically insulated. The electrolyte-uptake capability, porosity, and ionic conductivity of Celgard and PU/G/LiAc separators are shown in Table 1. The high porosity leads to high liquid-electrolyte uptake and high ionic conductivity. By comparison, the electrolyte uptake PU/G/LiAc separator is about three times higher than that of the Celgard separator, as well as the ionic conductivity does. Furthermore, the dissociated Li-ions from the PU/G/LiAc separator may improve the ionic conductivity of the separator/electrolyte system. Compared to the expensive commercial separator, the as-prepared composite separator here is composed of a low-cost PU matrix and a very small amount of graphene, which shows great potential for the battery application.

4. Conclusions: The PU/G/LiAc membrane prepared by an electrospinning technique was evaluated as a separator for high-performance LIBs. Besides the excellent electrochemical properties, the PU/G/LiAc separator also shows excellent wettability towards liquid electrolyte, as well as impressive thermal stability. Ionic conductivity of 2.47 $mS \cdot cm^{-1}$ can be obtained, indicating that the electrospun PU/G/LiAc membranes can be used as excellent performance separators.

5. Acknowledgments: The authors acknowledge financial support from the National Natural Science Foundation of China (grant nos. 51002128 and 21376199), Scientific Research Foundation of Hunan Provincial Education Department (grant no. 17A205), Natural Science Foundation of Hunan Province (grant no. 2018JJ2393), and Postgraduate Innovation Foundation of Hunan Province (grant no. XDCX2019B101).

6 References

[1] Yang H., Wu H.-H., Ge M., *ET AL.*: 'Simultaneously dual modification of Ni-rich layered oxide cathode for high-energy lithium-Ion batteries', *Adv. Funct. Mater.*, 2019, **23**, p. 1808825

[2] Li L., Xu M., Yao Q., *ET AL.*: 'Alleviating surface degradation of nickel-rich layered oxide cathode material by encapsulating with nanoscale Li-ions/electrons superionic conductors hybrid membrane for advanced Li-Ion batteries', *ACS Appl. Mater. Interfaces.*, 2016, **8**, pp. 30879–30889

[3] Duan J., Zhu C., Du Y., *ET AL.*: 'Synthesis of N-doped carbon-coated Zn–Sn mixed oxide cubes/graphene composite with enhanced lithium storage properties', *J. Mater. Sci.*, 2017, **52**, pp. 10470–10479

[4] Wei D., Zhong S., Zhang H., *ET AL.*: 'In situ construction of interconnected SnO2/nitrogen-doped carbon@TiO2 networks for lithium-ion half/full cells', *Electrochim. Acta*, 2018, **290**, pp. 312–321

[5] Li L., Yao Q., Liu J., *ET AL.*: 'Porous hollow superlattice NiMn(2)O(4)/NiCo(2)O(4) mesocrystals as a highly reversible anode material for lithium-ion batteries', *Front. Chem.*, 2018, **6**, pp. 153–153

[6] Chen H., Zhang W., Tang X.-Q., *ET AL.*: 'First principles study of P-doped borophene as anode materials for lithium ion batteries', *Appl. Surf. Sci.*, 2018, **427**, pp. 198–205

[7] Li L., Yao Q., Zhu H., *ET AL.*: 'Effect of Al substitution sites on $Li_{1-x}Al_x(Ni_{0.5}Co_{0.2}Mn_{0.3})1-yAl_yO_2$ cathode materials for lithium ion batteries', *J. Alloy. Compd.*, 2016, **686**, pp. 30–37

[8] Chen Z., Xu M., Zhu H., *ET AL.*: 'Enhanced electrochemical performance of polyacene coated LiMn2O3.95F0.05 for lithium ion batteries', *Appl. Surf. Sci.*, 2013, **286**, pp. 177–183

[9] Liang B., Liu Y., Xu Y.: 'Silicon-based materials as high capacity anodes for next generation lithium ion batteries', *J. Power Sour.*, 2014, **267**, pp. 469–490

[10] Li M., Liao Y., Liu Q., *ET AL.*: 'Application of poly(vinylidene fluoride-co-hexafluoropropylene) blended poly(methyl vinyl ether-alt-maleic anhydride) based gel polymer electrolyte by electrospinning in Li-ion batteries', *Solid State Ion.*, 2018, **325**, pp. 57–66

[11] Li H., Chen Y.-M., Ma X.-T., *ET AL.*: 'Gel polymer electrolytes based on active PVDF separator for lithium ion battery. I: preparation and property of PVDF/poly(dimethylsiloxane) blending membrane', *J. Membr. Sci.*, 2011, **379**, pp. 397–402

[12] Liang B., Jiang Q., Tang S., *ET AL.*: 'Porous polymer electrolytes with high ionic conductivity and good mechanical property for rechargeable batteries', *J. Power Sour.*, 2016, **307**, pp. 320–328

[13] Tang Y., Luo Z., Liu T., *ET AL.*: 'Effects of B2O3 on microstructure and ionic conductivity of Li6.5La3Zr1.5Nb0.5O12 solid electrolyte', *Ceram. Int.*, 2017, **43**, pp. 11879–11884

[14] Jiang Q., Liang B., Tang S., *ET AL.*: 'Preparation and performance of porous polymer electrolytes doped with nano-Al2O3', *J. Nanosci. Nanotechnol.*, 2018, **18**, pp. 1870–1875

[15] Jiang Y., Zhang P., Jin H., *ET AL.*: 'Flexible, nonflammable and Li-dendrite resistant Na2Ti3O7 nanobelt-based separators for advanced Li storage', *J. Membr. Sci.*, 2019, **583**, pp. 190–199

[16] Deng C., Jiang Y., Fan Z., *ET AL.*: 'Sepiolite-based separator for advanced Li-ion batteries', *Appl. Surf. Sci.*, 2019, **484**, pp. 446–452

[17] Jiang Y., Ding Y., Zhang P., *ET AL.*: 'Temperature-dependent on/off PVP@TiO2 separator for safe Li-storage', *J. Membr. Sci.*, 2018, **565**, pp. 33–41

[18] Liu X., Song K., Lu C., *ET AL.*: 'Electrospun PU@GO separators for advanced lithium ion batteries', *J. Membr. Sci.*, 2018, **555**, pp. 1–6

doi: 10.1049/mnl.2019.0164

[19] Wu Q.-Y., Liang H.-Q., Gu L., *ET AL.*: 'PVDF/PAN blend separators via thermally induced phase separation for lithium ion batteries', *Polymer*, 2016, **107**, pp. 54–60
[20] Tsao C.-H., Kuo P.-L.: 'Poly(dimethylsiloxane) hybrid gel polymer electrolytes of a porous structure for lithium ion battery', *J. Membr. Sci.*, 2015, **489**, pp. 36–42
[21] Costa C.M., Rodrigues L.C., Sencadas V., *ET AL.*: 'Effect of degree of porosity on the properties of poly(vinylidene fluoride–trifluorethylene) for Li-ion battery separators', *J. Membr. Sci.*, 2012, **407–408**, pp. 193–201
[22] Zhai Y., Wang N., Mao X., *ET AL.*: 'Sandwich-structured PVdF/PMIA/PVdF nanofibrous separators with robust mechanical strength and thermal stability for lithium ion batteries', *J. Mater. Chem. A*, 2014, **2**, pp. 14511–14518
[23] Khan W.S., Asmatulu R., Rodriguez V., *ET AL.*: 'Enhancing thermal and ionic conductivities of electrospun PAN and PMMA nanofibers by graphene nanoflake additions for battery-separator applications', *Int. J. Enery. Res.*, 2014, **38**, pp. 2044–2051
[24] Liang X., Yang Y., Jin X., *ET AL.*: 'The high performances of SiO2/Al2O3-coated electrospun polyimide fibrous separator for lithium-ion battery', *J. Membr. Sci.*, 2015, **493**, pp. 1–7
[25] Zhai Y., Xiao K., Yu J., *ET AL.*: 'Fabrication of hierarchical structured SiO2/polyetherimide-polyurethane nanofibrous separators with high performance for lithium ion batteries', *Electrochim. Acta.*, 2015, **154**, pp. 219–226
[26] Tong H., Tao X., Wu D., *ET AL.*: 'Preparation and characterization of doped TiO2 nanofibers by coaxial electrospining combined with sol–gel process', *J. Alloy. Compd.*, 2014, **586**, pp. 274–278
[27] Wen T.-C., Chen W.-C.: 'Gelled composite electrolyte comprising thermoplastic polyurethane and poly(ethylene oxide) for lithium batteries', *J. Power Sour.*, 2001, **92**, pp. 139–148
[28] Zhai Y., Xiao K., Yu J., *ET AL.*: 'Thermostable and nonflammable silica–polyetherimide–polyurethane nanofibrous separators for high power lithium ion batteries', *J. Mater. Chem. A*, 2015, **3**, pp. 10551–10558
[29] Wu N., Cao Q., Wang X., *ET AL.*: 'In situ ceramic fillers of electrospun thermoplastic polyurethane/poly(vinylidene fluoride) based gel polymer electrolytes for Li-ion batteries', *J. Power Sour.*, 2011, **196**, pp. 9751–9756
[30] Zhou L., Cao Q., Jing B., *ET AL.*: 'Study of a novel porous gel polymer electrolyte based on theromoplastic polyurethane/poly(vinylidene fluoride-co-hexafluoropropylene) by electrospinning technique', *J. Power Sour.*, 2014, **263**, pp. 118–124
[31] Knoche T., Lund R., Prymak O., *ET AL.*: 'Effect of annealing temperature on pore formation in preparation of advanced polyethylene battery separator membranes', *Mater. Today Commun.*, 2016, **8**, pp. 23–30
[32] Zainab G., Wang X., Yu J., *ET AL.*: 'Electrospun polyacrylonitrile/polyurethane composite nanofibrous separator with electrochemical performance for high power lithium ion batteries', *Mater. Chem. Phys.*, 2016, **182**, pp. 308–314